*Desalination and Water Treatment*
www.deswater.com

doi:10.5004/dwt.2018.22456

115 (2018) 45–52
May

# Citrate-coated magnetite nanoparticles as osmotic agent in a forward osmosis process

Raya Mohammed Kadhim[a,*], Entisar Eliwi Al-Abodi[b], Ahmed Faiq Al-Alawy[c]

[a]*Ministry of Health and Environment, Department of International Environment Relationships, Baghdad, Iraq, Tel. +9647809757554, email: chengraya@yahoo.com (R.M. Kadhim)*
[b]*College of Education Ibn Al-Haitham, Chemistry Department, University of Baghdad, Baghdad, Iraq, Tel. +9647709468906, email: entisaree2000@gmail.com (E.E. Al-Abodi)*
[c]*College of Engineering, Chemical Department, University of Baghdad, Baghdad, Iraq, Tel. +9647901205905, email: ahmedalalawy@yahoo.com (A.F. Al-Alawy)*

Received 14 December 2017; Accepted 3 May 2018

**ABSTRACT**

Iron oxide ($Fe_3O_4$) magnetic nanoparticles (MNPs) is the most promising draw solutes (DS) that have been studied during the past years. They gained their reputation because of the unique properties they possess, such as large surface area to volume ratio, magnetic properties, and the easiness of surface functionalization. Two samples of MNPs (MNPs-1 and MNPs-2) were synthesized by co-precipitation of ferric and ferrous ions in alkaline solution depending on certain parameters including pH, temperature, $Fe^{2+}/Fe^{3+}$ molar ratio, mixing rate, adding base to the reactants (and vice versa), and using $N_2$ gas. Tri-sodium citrate (TSC) was selected to functionalize the MNPs surface because of the carboxylate groups that it possesses. Hydrophilic citrate-coated magnetic nanoparticles (cit-MNPs) were obtained. The performance of cit-MNPs as DS was investigated by applying them in forward osmosis (FO) process with the use of cellulose triacetate (CTA) membrane. TSC was applied as DS to investigate the efficiency of cit-MNPs in comparison with it. Also, two types of salts were chosen for comparison with cit-MNPs, sodium chloride (NaCl) and sodium formate (HCOONa). The highest water fluxes obtained from MNPs-1, MNPs-2, TSC, NaCl and HCOONa at 2 g/l were 34.77, 28.41, 25.27, 24.6 and 30.67 LMH, respectively. All the results demonstrated that citrate-MNPs-1 performed better as DS.

*Keywords:* Forward osmosis; Draw solution; Citrate-coated magnetic nanoparticles; NaCl; Sodium formate

## 1. Introduction

Water shortage and lack of safe drinking water are the most serious challenges of the 21st century. The rapidly growing population and the accelerating increase in the standards of living have put stringent pressure on water and energy resources [1]. Looking for low energy consumption process for water production has been very urgent as the water crisis is the second worldwide concern [2]. Membrane processes are used for purification of polluted water resources, and that can strongly contribute to mitigation of water shortage. The recently resurgent forward osmosis process is one of the most important membrane processes which recognized as promising approach to water treatment applications [3] due to their low energy consumption, low membrane fouling tendency and high selectivity [4]. FO process has the potential to become a sustainable alternative to conventional membrane processes [5]. It has been studied in a variety of research fields including, desalination for potable [6] and non-potable [7] water purposes, water treatment [8], wastewater treatment [9], pharmaceutical applications [8], food processing [10], osmotic power generation [11], and pre-treatment for RO desalination [12].

*Corresponding author.

Choosing appropriate DS for the FO process is of key importance. An effective DS should generate enough osmotic pressure, its reverse flux should be minimal, would not degrade the membrane chemically nor physically, with low molecular weight, be easily and economically recycled and separated from the permeate to obtain purified water and to be reused, and also it should be nontoxic, stable and affordable [13]. Many types of draw solutes have been used in FO process to investigate their efficiency, such as inorganic salts [14], organic solutes [15,16], hydrogels [17], polyelectrolytes [18], or solvents with a switchable polarity [19,20]. However, the use of many types of these DS in FO is limited due to many reasons, such as relatively low osmotic pressure, the difficult and energy consuming separating processes from the permeate, the formation of toxic thermolytic products, and the inability to reuse the materials [21].

Magnetic nanoparticles have drawn a lot of attention in many applications during the past years due to their unique characteristics, such as large surface area to volume ratio, magnetic properties and easy surface functionalization. The properties of nanoparticles are remarkably different from small molecules and their chemistry and synthesis imposes that they be considered more like complex mixtures than small molecules [22]. The magnetic properties of MNPs enable the manipulation of these particles by applying an external magnetic field. Ling et al. [23] and Ge et al. [24] have developed hydrophilic MNPs as DS in FO process by taking advantage of the aforementioned characteristics. They used magnetic separator to collect MNPs and easily separate them from the permeate to obtain pure water as well as to reuse them efficiently which minimizes the overall cost of the operation. MNPs are also can be collected by conventional membrane processes such as nanofiltration (NF) or ultrafiltration (UF) [25,26]. FO membranes can intercept MNPs entirely because the pore size of the membrane is smaller than the size of the particles [23]. Ling et al. used hydrophilic MNPs to desalinate both seawater and brackish water and they believed that MNPs can be a promising technology to reclaim water from wastewater [25].

The magnetic properties of MNPs depend on their size and their size may be influenced by many factors, such as pH of the solution [27,28], ($Fe^{2+}/Fe^{3+}$) molar ratio, type of iron salts (chlorides, nitrates, sulfate... etc.) [29], temperature of the reaction [30], presence of oxygen [31,32,33], and mixing rate [34]. The nanoparticle size in turn influences the osmotic performance of the DS because small size particles provide large surface area and subsequently more coating substance will be obtained per volume which means higher osmotic pressure and as a result higher flux. However, the small size also reduces the magnetic properties [35] which makes the recovery of smaller diameter MNPs unsatisfactory because their diameters jump out of the range that the magnetic field can capture [23]. Magnetic nanoparticles, magnetite ($Fe_3O_4$) in specific, can be synthesized by various methods, including: ultrasound irradiation [36], sol-gel [37], thermal decomposition [38] and co-precipitation [39,40].

Co-precipitation is the most commonly used method. It is simple, inexpensive and effective chemical path to prepare MNPs. It can be explained as the co-precipitation of ferric and ferrous ions in alkaline solution. Chemical co-precipitation can yield high-purity, fine particles of single and multicomponent metal oxides and the reaction is fast. $Fe_3O_4$ crystals can be seen directly after mixing alkaline with the iron salts [41].

The zeta potential can be defined as the electrostatic potential at the boundary dividing the compact layer and the diffuse layer of the colloidal particles [42]. It is a measure of the stability of nanoparticles (NPs) suspensions. The higher electric charge on the surface of the NPs the more they will be stable and safe from being agglomerated in solution and that ensures easy redispersion because of the strong repulsive forces among particles [43]. As a rule of thumb, absolute zeta potential values over 30 mV give good stability and over 60 mV excellent stability, while about 20 mV sustain only short term stability. Values in the range –5 mV to +5 mV indicate fast aggregation [44,45]. MNPs are known to have the tendency to aggregate to minimize their surface energy due to their ultra-small size and large surface area. However, NP dispersions can be stabilized by the use of a suitable surface coating. Also the surface coating can function the NPs with new properties, such as high osmotic pressure in case the coating material have hydrophilic groups [25].

Citrate is one of the products from the tricarboxylic acid cycle (TAC), a normal metabolic process in the human body. It is chiefly used as a food additive, usually for flavor or as a preservative, and in drugs too. It is recognized as safe for use in food and drugs by all main international food regulatory agencies. Citrate possess three hydrophilic-COOH groups; therefore, it can easily bind to iron oxide through chemisorption process [46]. The chemisorption can assure electrostatic stabilization of the interaction forces preventing the agglomeration susceptibility of the MNPs [47]. By binding to the surface of MNPs, citrate acts as a surfactant to form a stable dispersion of MNPs in aqueous solution, and at the same time endows the particle surfaces with carboxylate functional groups which enhances the interaction between water and MNPs [48].

In the current work, magnetic nanoparticles were synthesized and coated with trisodium citrate (TSC) to obtain cit-MNPs. Cit-MNPs efficiency as draw solutes were investigated in FO process with the use of CTA membrane. Their efficiency was compared to the efficiency of trisodium citrate salt alone. Also, a comparison is made with two different salts (organic and inorganic), sodium chloride and sodium formate.

## 2. Experimental Work

### 2.1. Materials

Hydrochloric acid (HCl, 37%) from ROMIL-SA, iron(III) chloride anhydrous ($FeCl_3$, ≥97%) from Sinopharm Chemical, iron(II) sulphate heptahydrate ($FeSO_4{\cdot}7H_2O$, 98%), Tri-sodium citrate dihydrate ($Na_3C_6H_5O_7{\cdot}2H_2O$) and Sodium formate (HCOONa, 98%) from BDH Chemicals (England), Sodium hydroxide (NaOH, 99%) from Applichem GmbH (Germany). The distilled water used in all experiments was produced from GFL - Gesellschaft für Labortechnik water distillation unit (Germany).

### 2.2. Preparation of citrate-coated magnetic nanoparticles

Magnetic nanoparticles $Fe_3O_4$ were synthesized by the co-precipitation of ferric and ferrous ions in alkaline solu-

tion under different preparation conditions, according to the literature [49,50]. In the first method, MNPs-1 were prepared by using nitrogen only to deoxygenate the distilled water used for dissolving $Fe^{2+}$ and $Fe^{3+}$ salts and not throughout the whole process of synthesis of MNPs. The process happened at room temperature and the iron salts solution was added to the base. In the second method, MNPs-2 were prepared at 80°C without the use of nitrogen at any point during the process. The base was added to the iron salts solution. Then, both synthesized MNPs-1 and MNPs-2 were coated with TSC (Fig. 1 shows the structural formula) to obtain cit-MNPs-1 and cit-MNPs-2, respectively according to literature [48]. The citrate works on stabilizing MNPs by providing hydrophilic functional groups to their surface. 4 g of bare MNPs dispersed in 200 mL of distilled water, and 4.85 g of tri-sodium citrate dihydrate dissolved in 10 mL of distilled water were added together with vigorous and continuous stirring at 95°C for 60 min. The resulting solution was centrifuged at 10,000 rpm for 30 min to remove the reaction solvent. The supernatant was removed and the precipitate was redispersed in 200 mL of distilled water and ultra sonicated for 20 min. The resulted product was cit-MNPs. The precipitate of cit-MNPs was isolated from the supernatant then dried using dryer at 50°C for 4 h.

### 2.3. Characterization of Citrate-Coated MNPs

The prepared MNPs were characterized with XRD to verify the magnetite phase and also to determine the crystalline size. They were also characterized by SEM, according to former paper, which images showed spherical particles shape. Fourier transform infrared FTIR analysis were performed on cit-MNPs using a IRPrestige-21 Fourier-transform infrared spectrophotometer/ shimadzu, Japan (scan range from 7800 to 350 $cm^{-1}$) to confirm that the MNPs were coated with citrate. The spectra were obtained by pressing MNPs into KBr pellets. The zeta-potential of the MNPs was measured with Zeta potential Analyzer, Zeta Plus/ Brookhaven, USA (zeta potential range: –150 to +150 mV) to prove the hydrophilicity of the synthesized cit-MNPs by estimating their stability. AFM, SPM-AA3000 Angstrom Advanced Inc., Scanning Probe Microscope, USA was used to determine the average particle size and the particle size distribution of MNPs. The osmotic pressure of the draw solutions was measured using KNAUER, K-7400 Semimicro Osmometer, Germany. This device uses the technique of freezing-point depression to measure osmolality (mOsmol/Kg), which is the concentration of a solution expressed as the total number of solute particles per kg.

### 2.4. Forward osmosis process

A lab-scale FO unit assembled in the laboratory of Chemical Engineering Department/University of Baghdad was used in the experiments. Fig. 2 illustrates a picture of the FO unit. Cellulose triacetate (CTA) membrane (Hydration Technology Innovation (HTI), USA) was used as FO membrane with FO mode (where the support layer of the membrane faces the draw solution and the active layer faces the feed solution). On each side of the membrane, side stream mode identical two cell parts were designed in a side stream configuration with a rectangular channel of 14 cm length, 10 cm width and 0.5 cm depth. Draw and feed solutions where co-currently flowing through the channel of the cell and their velocities were maintained at 3 L/min during the FO testing with 0.2 bar inlet pressure at the feed side. The water permeation flux ($J_w$, $L{\cdot}m^{-2}{\cdot}h^{-1}$, abbreviated as LMH) was calculated from the change in volume of the feed solution as below.

$$J_w = \frac{\Delta V}{(A * \Delta t)} \quad (1)$$

where $\Delta V$ (L) is the permeated water collected during specific time $\Delta t$ (h) in the FO process run, and $A$ is the membrane effective surface area ($m^2$).

During all experiments, the temperature range was (38–42°C), and distilled water was used as feed solution (FS). The prepared cit-MNPs was used as draw solution. Two concentrations for each type of cit-MNPs were applied, 0.5 and 2 g/L. The cit-MNPs draw solution was prepared by dissolving certain amounts of the MNPs in water according to the desired concentration. The reverse flux of MNPs during FO tests observed to be almost negligible and this is consistent with Ling et al. [23]. To investigate the efficiency of cit-MNPs as DS, 2 g/L of standalone citrate salt was applied in FO for comparison. Also, to compare the performance of cit-MNPs as draw solute with other conventional draw solutes, NaCl and HCOONa were used with 2 g/L concentration of each salt, and each one in a different run.

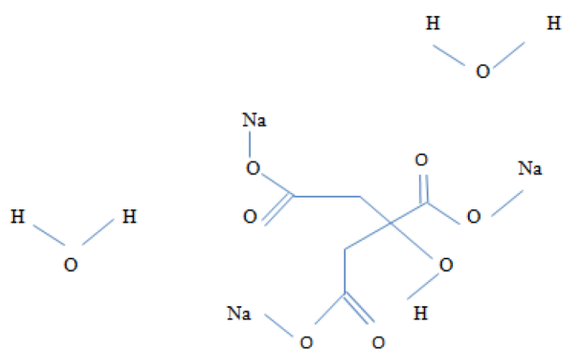


Fig. 1. Structural formula of TSC dihydrate.

Fig. 2. FO unit with cit-MNPs as draw solution.

## 3. Results and discussion

### 3.1. Characterization of citrate-coated MNPs

To prove the formation of magnetite phase, X-ray diffractometer (XRD) was used. The patterns of x-ray diffraction of MNPs-1 and MNPs-2 indicated a highly crystalline structure for magnetite ($Fe_3O_4$). According to Scherrer's equation, the crystalline size of MNPs-1 and MNPs-2 were 14.3 nm and 13.8 nm, respectively.

FTIR spectra was performed to confirm that surface functional groups from citrate have been attached to the iron oxide surface. Fig. 3 shows the FTIR spectra of the functionalized MNPs-1 and MNPs-2. The strong Fe-O absorption bands around 600 $cm^{-1}$ verifies that the main phase of the synthesized nanoparticles is $Fe_3O_4$. This characteristic peaks can be attributed to the lattice absorption of iron oxide [51]. A large and intense band from 3230 to 3450 $cm^{-1}$ (for cit-MNPs-1) and 3450 $cm^{-1}$ (for cit-MNPs-2) could be ascribed to the structural OH groups as well as to the attendance of non-dissociated O-H groups of citrate and traces of water [47]. Two new absorption peaks at 1388 and 1587 $cm^{-1}$ (for cit-MNPs-1), and 1377 and 1585 $cm^{-1}$ (for cit-MNPs-2) appear in the FTIR spectra of cit-MNPs, which are distinctive of the carboxylate functional group [52]. The vibrational mode appearing at 1388 and 1377 $cm^{-1}$ (aforementioned) can be attributed to the symmetric stretching of a citrate $COO^-$ group. The peak at 1600 $cm^{-1}$ is assignable to the C=O vibration in citrate switches to an intense band at about 1587 and 1585 $cm^{-1}$ for cit-MNPs-1 and cit-MNPs-2, respectively [53]. This confirms the binding of citrate to the surface of magnetite by chemisorption of carboxylate ions.

The results of AFM showed that cit-MNPs-1 and cit-MNPs-2 are convergent in size with (69.54) and (66.08) nm, respectively. Fig. 4 illustrates AFM picture of cit-MNPs-1, cit-MNPs-2 and the particle size distribution of both. The surface charges of the cit-MNPs-1 and cit-MNPs-2 were

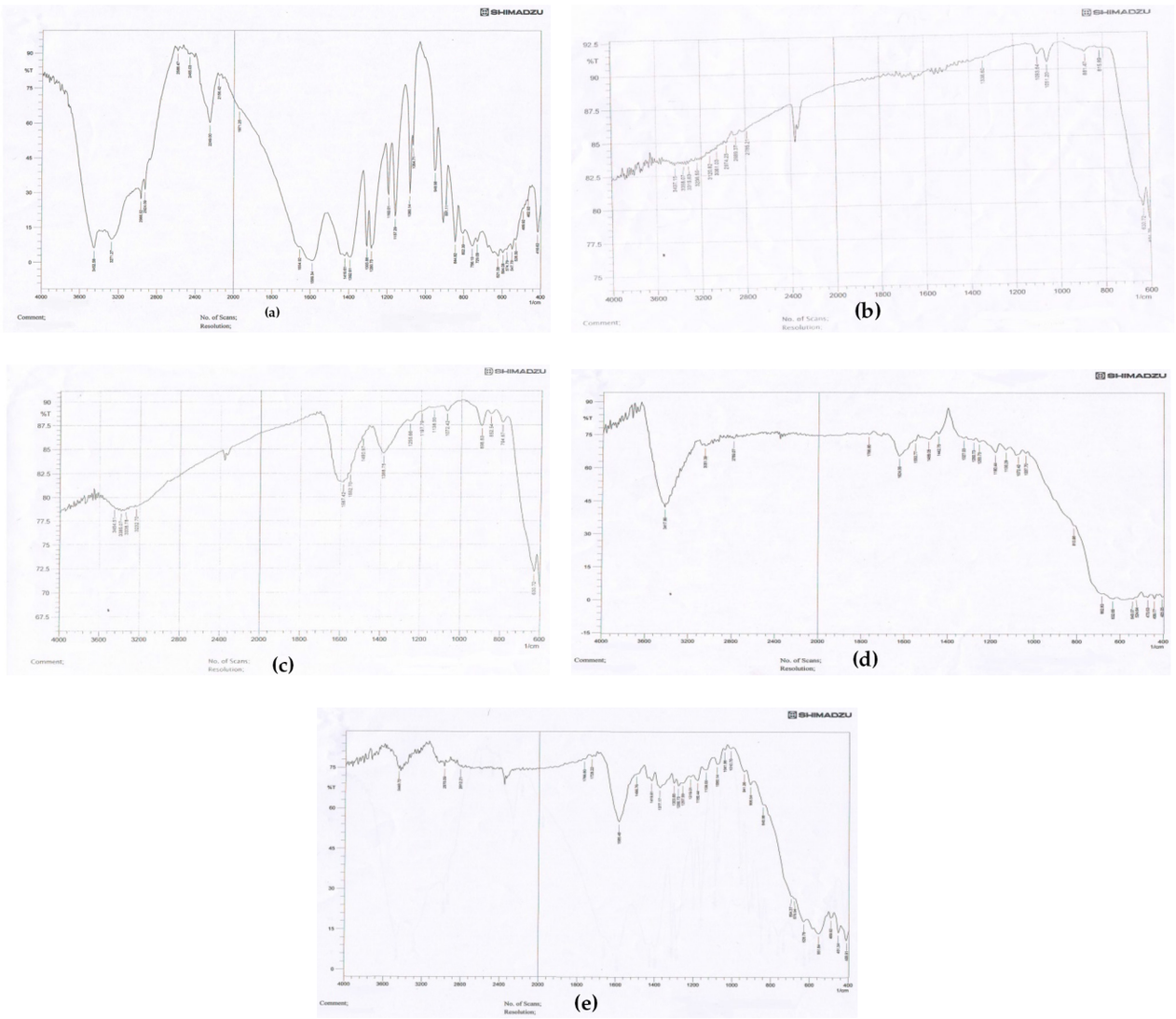


Fig. 3. FTIR spectra for (a) pure TSC (b) MNPs-1 (c) cit-MNPs-1 (d) MNPs-2 (e) cit-MNPs-2.

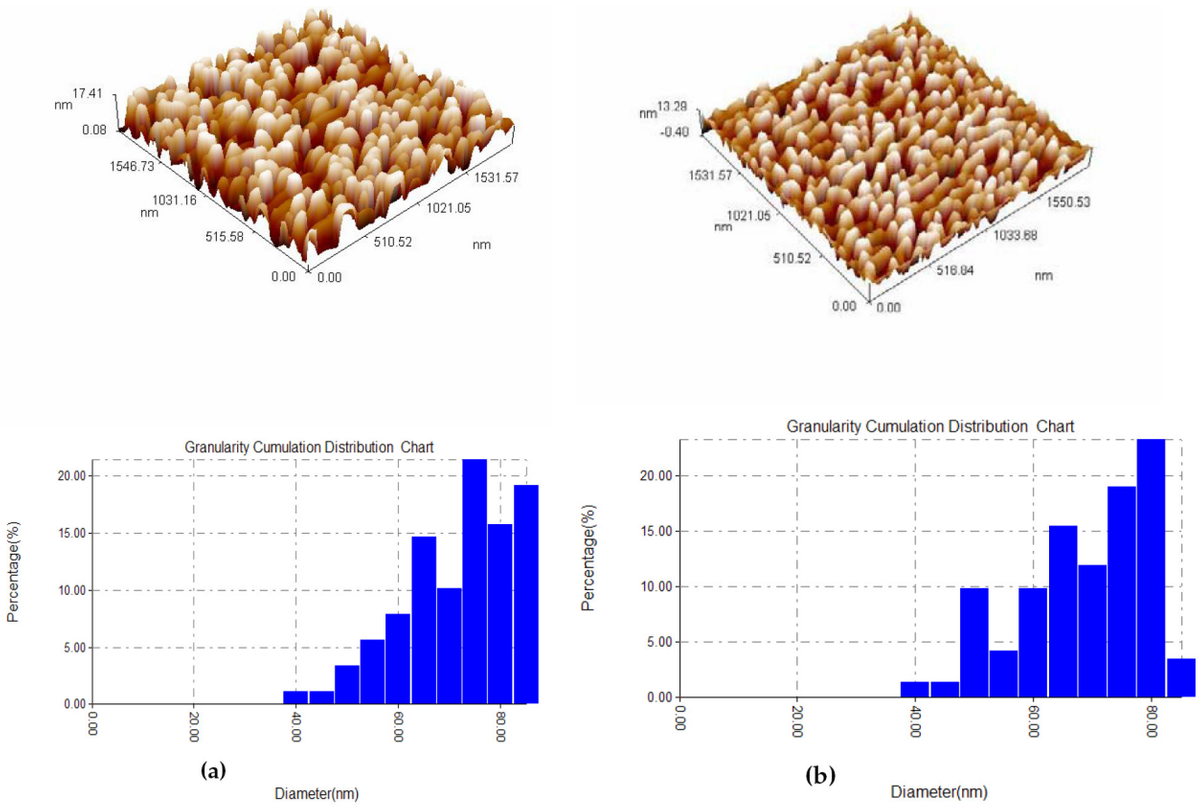


Fig. 4. AFM (a) image and particle size distribution of cit-MNPs-1 (b) image and particle size distribution of cit-MNPs-2.

measured by zeta potential analysis and the results gave values of (–33.67) and (–20.75) mV, respectively. From these results we can predict better performance for cit-MNPs-1 than cit-MNPs-2 because the latter has less absolute zeta potential value, which means less stability and faster agglomeration. The osmotic pressure was measured by the osmometer for all the cit-MNPs samples used in experiments of this work. All the results were either out of range or freeze before the measuring time out (error). This might be because this type of devices are not designed to measure the osmotic pressure of such colloidal solutions of MNPs, while it can measure the osmotic pressure of brine solutions (ionic solutions). The osmolalities of the 2 g/L TSC, NaCl and HCOONa solutions measured by the osmometer were 23, 68 and 56 mOsmole, respectively.

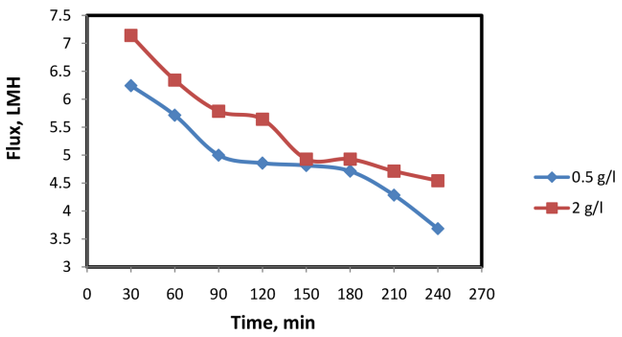


Fig. 5. Water flux as a function of time for cit-MNPs-1.

### 3.2. Performance of citrate-coated MNPs as draw solute

Two concentrations of both cit-MNP-1 and cit-MNPs-2 were applied in the experiments, 0.5 and 2 g/L. Each experiment duration lasted for 3–4 h with feed and draw solutions flow rate of 3 L/min. Distilled water was used as feed solution through all experiments. Figs. 5 and 6 show the FO water flux as a function of time for cit-MNPs-1 and cit-MNPs-2. From both figures, we notice that the flux decreases with time and the decline in the curve is stronger during the first two hours than the last two hours. This can be attributed to the dilution happens to the DS through time as a result of the mixing of the permeate water with it.

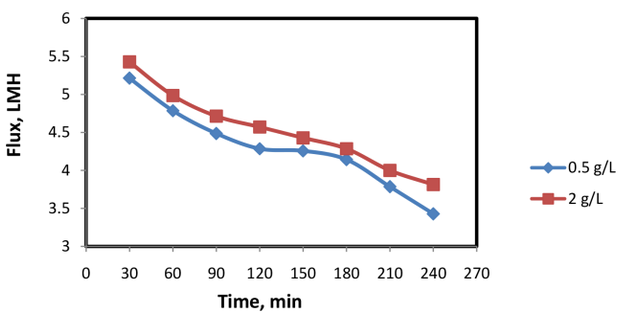


Fig. 6. Water flux as a function of time for cit-MNPs-2.

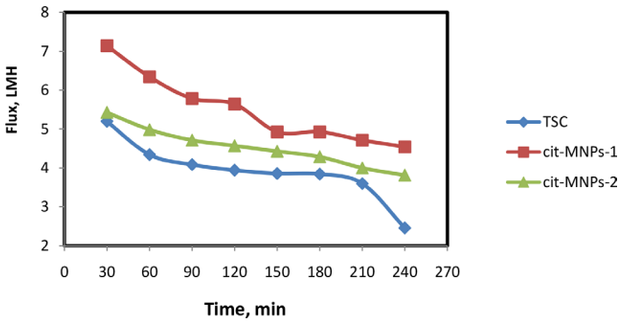


Fig. 7. Water flux as a function of time for cit-MNPs-1, cit-MNPs-2 and TSC.

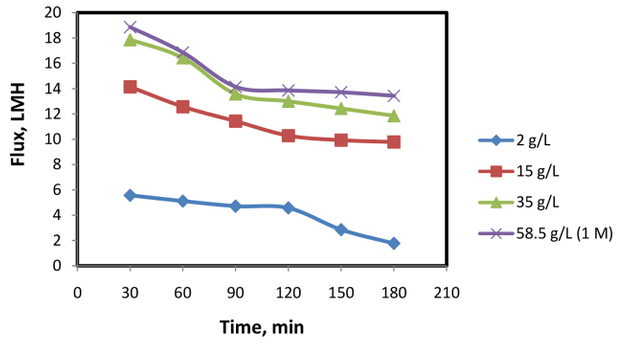


Fig. 8. Water flux as a function of time for NaCl.

Another explanation is that the decrease in the efficiency of cit-MNPs ascribed to the agglomeration happens to them over time. Also, the flux increases with the increase of concentration of the DS because osmotic pressure of the DS increases which means higher driving force. On the other hand, the performance of cit-MNPs-1 is observed to be better than the performance of cit-MNPs-2. This can be ascribed to the higher stability of the first type which is confirmed by the zeta potential measurements. Fig. 7 shows a comparison between cit-MNPs and TSC salt at concentration of 2 g/L. The results prove that cit-MNPs perform better as DS in FO process than TSC alone due to the large surface area to volume ratio, which endows MNPs with higher osmotic pressure, and hence better performance as DS. Cit-MNPs can be regenerated by applying external magnetic field and reused.

Sodium chloride and sodium formate were used as DS in FO process. Figs. 8 and 9 show the water flux as a function of time of NaCl and HCOONa, respectively, at 4 different concentrations for each salt. The same behavior as in Figs. 5 and 6 can be seen here. Furthermore, NaCl gave higher water flux than HCOONa due to higher solute diffusion coefficient and lower molecular weight of NaCl that gives higher osmotic pressure, i.e., higher driving force. To compare the performance of cit-MNPs as DS with these two salts, 2 g/L of each was selected as DS concentration. Fig. 10 shows the FO water flux of NaCl and HCOONa in comparison with the same concentration of both types of cit-MNPs. Obviously, cit-MNPs-1 is more efficient than all other types at the same conditions. The highest water flux obtained

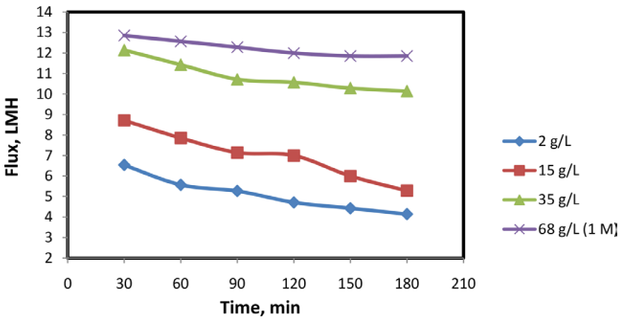


Fig. 9. Water flux as a function of time for HCOONa.

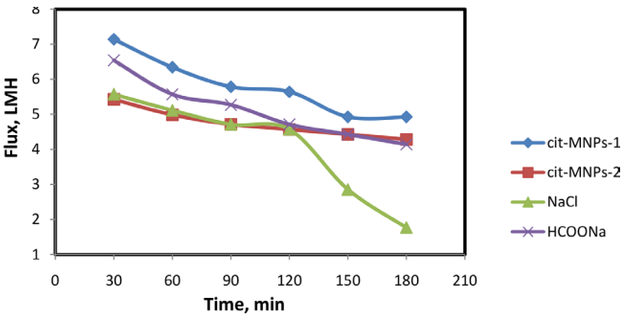


Fig. 10. Water flux as a function of time for cit-MNPs-1, cit-MNPs-2, NaCl and HCOONa.

Table 1
Water fluxes of different used draw solutions (time = 3 h)

| Draw solution | Water flux (LMH) |
|---|---|
| | 2 (g/l) |
| Cit-MNPs-1 | 34.77 |
| Cit-MNPs-2 | 28.41 |
| NaCl | 24.60 |
| HCOONa | 30.67 |

from cit-MNPs-1, cit-MNPs-2, NaCl and HCOONa are 7.14, 5.42, 5.57 and 6.54 LMH, respectively. However, cit-MNPs-2 and NaCl had nearly the same water flux during the first two hours. Then, a sharp decline in the flux is observed in NaCl performance during the next hour. This means that cit-MNPs-2 conserve a more uniform and stable performance than NaCl and kept giving more flux during the third hour. On the other hand, HCOONa gave better performance than cit-MNPs-2 until the last 30 min where it gave less flux than cit-MNPs-2. By aggregating the water fluxes through 3 h run, we obtain the results showed in Table 1.

## 4. Conclusions

In this study, MNPs have been synthesized by co-precipitation method under different preparation conditions, and coated with tri-sodium citrate (TSC). Cit-MNPs-1 and cit-MNPs-2 were obtained with particle size of (69.54) and

(66.08) nm, respectively. The zeta potential measurements were (–33.67) and (–20.75) mV for cit-MNPs-1 and cit-MNPs-2, respectively. Cit-MNPs-1 performed better than cit-MNPs-2 as DS in FO process because of their higher stability dispersion. Both are more efficient than TSC alone. On the other hand, cit-MNPs-1 showed higher water flux in comparison with NaCl and HCOONa. In spite of the fact that cit-MNPs-2 gave lower flux than HCOONa, they showed equal fluxes at the fourth hour of the run. Cit-MNPs conserve a more uniform performance than conventional salts as DS. The water fluxes of the used draw solutions in the current work were in the following order:

cit-MNPs-1 > HCOONa > cit-MNPs-2 >TSC > NaCl

## Recommendations

For future work, we recommend the following:

1. Study the efficiency of cit-MNPs as DS in FO process for longer runs like 5 or 6 hours of operation to investigate their performance after this period of time.
2. Study the efficiency of cit-MNPs with different types of feed solutions such as seawater, heavy metals or oily waste water.
3. Investigate the effect of cit-MNPs on membrane fouling.
4. Study different DS recovery processes, such as magnetic field or UF, and their effect on the efficiency of MNPs after recycling.

## Symbols

$J_w$ — The water permeation flux ($L \cdot m^{-2} \cdot h^{-1}$, abbreviated as LMH)
$\Delta V$ — The permeated water volume (L)
$\Delta t$ — The time during which the permeate water collected (h)
$A$ — Membrane effective surface area ($m^2$)

## References


[1] R.L. McGinnis, M. Elimelech, Global challenges in energy and water supply: the promise of engineered osmosis, Environ. Sci. Technol., 42 (2008) 8625–8629.
[2] M.A. Shannon, P.W. Bohn, M. Elimelech, J.G. Georgiadis, B.J. Mariñas, A.M. Mayes, Science and technology for water purification in the coming decades, Nature, 452 (2008) 301–310.
[3] D.L. Shaffer, J.R. Werber, H. Jaramillo, S. Lin, M. Elimelech, Forward osmosis: Where are we now?, Desalination, 356 (2015) 271–284.
[4] T.-S. Chung, S. Zhang, K.Y. Wang, J. Su, M.M. Ling, Forward osmosis processes: Yesterday, today and tomorrow, Desalination, 287 (2012) 78–81.
[5] B. Mi, M. Elimelech, Organic fouling of forward osmosis membranes: Fouling reversibility and cleaning without chemical reagents, J. Membr. Sci., 348 (2010) 337–345.
[6] T.-S. Chung, X. Li, R.C. Ong, Q. Ge, H. Wang, G. Han, Emerging forward osmosis (FO) technologies and challenges ahead for clean water and clean energy applications, Curr. Opin. Chem. Eng., 1 (2012) 246–257.
[7] L.A. Hoover, W.A. Phillip, A. Tiraferri, N.Y. Yip, M. Elimelech, Forward with osmosis: emerging applications for greater sustainability, Environ. Sci. Technol., 45 (2011) 9824–9830.
[8] T.Y. Cath, A.E. Childress, M. Elimelech, Forward osmosis: Principles, applications, and recent developments: review, J. Membr. Sci., 281 (2006) 70–87.
[9] R.W. Holloway, A.E. Childress, K.E. Dennett, T.Y. Cath, Forward osmosis for concentration of anaerobic digester centrate, Water Res., 41 (2007) 4005–4014.
[10] E.M. Garcia-Castello, J.R. McCutcheon, Dewatering press liquor derived from orange production by forward osmosis, J. Membr. Sci., 372 (2011) 97–101.
[11] Q. She, X. Jin, C.Y. Tang, Osmotic power production from salinity gradient resource by pressure retarded osmosis: Effects of operating conditions and reverse solute diffusion, J. Membr. Sci., 401–402 (2012) 262–273.
[12] O.A. Bamaga, A. Yokochi, E.G. Beaudry, Application of forward osmosis in pretreatment of seawater for small reverse osmosis desalination units, Desalination and Water Treat., 5 (2009) 183–191.
[13] J.R. McCutcheon, R.L. McGinnis, M. Elimelech, A novel ammonia-carbon dioxide forward (direct) osmosis desalination process, Desalination, 174 (2005) 1–11.
[14] A. Achilli, T.Y. Cath, A.E. Childress, Selection of inorganic-based draw solutions for forward osmosis applications, J. Membr. Sci., 364 (2010) 233–241.
[15] J.O. Kessler, C.D. Moody, Drinking water from sea water by forward osmosis. Desalination, 18 (1976) 297–306.
[16] N.T. Hau, S.S. Chen, N.C. Nguyen, K.Z. Huang, H.H. Ngo, W.S. Guo, Exploration of EDTA sodium salt as novel draw solution in forward osmosis process for dewatering of high nutrient sludge, J. Membr. Sci., 455 (2014) 305–311.
[17] D. Li, X. Zhang, J. Yao, G.P. Simon, H. Wang, Stimuli-responsive polymer hydrogels as a new class of draw agent for forward osmosis desalination, Chem. Commun., 47 (2011) 1710–1712.
[18] Q. Ge, J. Su, G.L. Amy, T.-S. Chung, Exploration of polyelectrolytes as draw solutes in forward osmosis processes, Water Res., 46 (2012) 1318–1326.
[19] M.L. Stone, C. Rae, F.F. Stewart, A.D. Wilson, Switchable polarity solvents as draw solutes for forward osmosis, Desalination, 312 (2013) 124–129.
[20] A.D. Wilson, F.F. Stewart, Structure-function study of tertiary amines as switchable polarity solvents, RSC Adv., 4 (2014) 11039–11049.
[21] C. Klaysom, T.Y. Cath, T. Depuydt, I.F.J. Vankelecom, Forward and pressure retarded osmosis: potential solutions for global challenges in energy and water supply, Chem. Soc. Rev., 42 (2013) 6959–6989.
[22] P. Christian, F. Von der Kammer, M. Baalousha, T.h. Hofmann, Nanoparticles: structure, properties, preparation and behavior in environmental media, Ecotoxicology, 17 (2008) 326–343.
[23] M.M. Ling, K.Y. Wang, T.-S. Chung, Highly water soluble magnetic nanoparticles as novel draw solutes in forward osmosis for water reuse, Ind. Eng. Chem. Res., 49 (2010) 5869–5876.
[24] Q.C. Ge, J.C. Su, T.S. Chung, G. Amy, Hydrophilic super paramagnetic nanoparticles: synthesis, characterization, and performance in forward osmosis processes, Ind. Eng. Chem. Res., 50 (2011) 382–388.
[25] M.M. Ling, T.-S. Chung, Desalination process using super hydrophilic nanoparticles via forward osmosis integrated with ultrafiltration regeneration, Desalination, 278 (2011) 194–202.
[26] T. Alejo, M. Arruebo, V. Carcelen, V.M. Monsalvo, V. Sebastian, Advances in draw solutes for forward osmosis: Hybrid organic-inorganic nanoparticles and conventional solutes, Chem. Eng. J., 309 (2017) 738–752.
[27] L. Vayssie`res, C. Chane´ac, E. Tronc, J.-P. Jolivet, Size tailoring of magnetite particles formed by aqueous precipitation: An example of thermodynamic stability of nano metric oxide particles, J. Colloid Interface Sci., 205 (1998) 205–212.
[28] W. Jiang, H.C. Yang, S.Y. Yang, H.E. Horng, J.C. Hung, Y.C. Chen, C.Y. Hong, Preparation and properties of super paramagnetic nanoparticles with narrow size distribution and biocompatible, J. Magn. Magn. Mater., 283 (2004) 210–214.

[29] L. Babes, B. Denizot, G. Tanguy, J.J. Le Jeune, P. Jallet, Synthesis of iron oxide nanoparticles used as MRI contrast agents: a parametric study, J. Colloid Interface Sci., 212 (1999) 474–482.
[30] M. Mahdavi, M.B. Ahmad, M.J. Haron, F. Namvar, B. Nadi, M.Z. Ab Rahman, J. Amin, Synthesis, surface modification and characterisation of biocompatible magnetic iron oxide nanoparticles for biomedical applications, Molecules, 18 (2013) 7533–7548.
[31] D.K. Kim, Y. Zhang, W. Voit, K.V. Rao, M.J. Muhammed, Synthesis and characterization of surfactant-coated super paramagnetic mono dispersed iron oxide nanoparticles, J. Magn. Magn. Mater., 225 (2001) 30–36.
[32] A.K. Gupta, S. Wells, Surface-modified super paramagnetic nanoparticles for drug delivery: preparation, characterization, and cytotoxicity studies, IEEE Trans. Nano Biosci., 3 (2004) 66–73.
[33] A. Khan, Preparation and characterization of magnetic nanoparticles embedded in micro gels, Mater. Lett., 62 (2008) 898–902.
[34] J. Sun , S. Zhou, P. Hou, Y. Yang, J. Weng, X. Li, M. Li, Synthesis and characterization of biocompatible $Fe_3O_4$ Nanoparticles, J. Biomed. Mater. Res. Part. A, 10 (2006) 333–341.
[35] T. Mishra, S. Ramola, A.K. Shankhwar, R.K. Srivastava, Use of synthesized hydrophilic magnetic nanoparticles (HMNPs) in forward osmosis for water reuse, Water Sci. Technol. Water Supply, 16 (2016) 229–236.
[36] B.M. Teo, F. Chen, T.A. Hatton, F. Grieser, M. Ashok kumar, Novel one-pot synthesis of magnetite latex nanoparticles by ultrasound irradiation, Langmuir, 25 (2009) 2593–2595.
[37] A.S. Teja, P.-Y. Koh, Synthesis, properties, and applications of magnetic iron oxide nanoparticles, Prog. Cryst. Growth Charact. Mater., 55 (2009) 22–45.
[38] J.M. Vargas, R.D. Zysler, Tailoring the size in colloidal iron oxide magnetic nanoparticles, Nano technology, 16 (2005) 1474–1476.
[39] S. Qu, H. Yang, D. Ren, S. Kan, G. Zou, D. Li, M. Li, Magnetite nanoparticles prepared by precipitation from partially reduced ferric chloride aqueous solutions, J. Colloid Interf. Sci., 215 (1999) 190–192.
[40] I. Nedkov, T. Merodiiska, L. Slavov, R.E. Vandenberghe, Y. Kusano, J. Takada, Surface oxidation, size and shape of nanosized magnetite obtained by coprecipitation, J. Magn. Magn. Mater., 300 (2006) 358–367.
[41] S. Chen, J. Feng, X. Guo, J. Hong, W. Ding, One-step wet chemistry for preparation of magnetite nano rods, Mater. Lett., 59 (2005) 985–988.
[42] I. Ostolska, M. Wiśniewska, Application of the zeta potential measurements to explanation of colloidal $Cr_2O_3$ stability mechanism in the presence of the ionic polyamino acids, Colloid Polym. Sci., 292 (2014) 2453–2464.
[43] S. Honary, F. Zahir, Effect of zeta potential on the properties of nano-drug, J. Pharmaceutical Research, 12 (2013) 265–273.
[44] C. Jacobs, O. Kayser, R.H. Müller, Nano suspensions as a new approach for the formulation for the poorly soluble drug tarazepide, Int. J. Pharm., 196 (2000) 161–164.
[45] S.A. Wissing, O. Kayser, R.H. Müller, Solid lipid nanoparticles for parenteral drug delivery, Adv. Drug Delivery Rev., 56 (2004) 1257–1272.
[46] N. Kallay, E. Matijevic, Adsorption at solid/solution interfaces. 1. Interpretation of surface complexation of oxalic and citric acids with hematite, Langmuir, 1 (1985) 195–201.
[47] M. Răcuciu, Synthesis protocol influence on aqueous magnetic fluid properties, Curr. Appl. Phys., 9 (2009) 1062–1066.
[48] Y. Na, S. Yang, S. Lee, Evaluation of citrate-coated magnetic nanoparticles as draw solute for forward osmosis, Desalination, 347 (2014) 34–42.
[49] Y.S. Kang, S. Risbud, J.F. Rabolt, P. Stroeve, Synthesis and characterization of nanometer-size $Fe_3O_4$ and $\gamma$-$Fe_2O_3$ particles, Chem. Mater., 8 (1996) 2209–2211.
[50] H.K. Al-Hakeim, F.F.M. Al-Kazaz, H.K.A. Alobaid, Adsorption of LH, FSH, and TSH on magnetic nanoparticles, J. Bionano Sci., 9 (2015) 1–9.
[51] W. Cai, J.Q. Wan, Facile synthesis of super paramagnetic magnetite nanoparticles in liquid polyols, J. Colloid Interface Sci., 305 (2007) 366–370.
[52] A. Goodarzi, Y. Sahoo, M.T. Swihart, P.N. Prasad, Aqueous ferrofluid of citric acid coated magnetite particles, Mater. Res. Soc. Symp. Proc., 789 (2004) 129–134.
[53] Y. Sahoo, A. Goodarzi, M.T. Swihart, T.Y. Ohulchanskyy, N. Kaur, E.P. Furlani, P.N. Prasad, Aqueous ferrofluid of magnetite nanoparticles: fluorescence labeling and magnetophoretic control, J. Phys. Chem. B, 109 (2005) 3879–3885.